International Journal of
INTELLIGENT SYSTEMS AND APPLICATIONS IN ENGINEERING

ISSN:2147-6799 www.ijisae.org Original Research Paper

Characterization of The Fourth-Order S-curve Trajectory Using Unitization Method

Rupesh Tatte*[1], Hemant Jawale[2], Hemant Thorat[3]

Submitted: 27/01/2024 **Revised**: 05/03/2024 **Accepted**: 13/03/2024

Abstract: In point-to-point motion transfer applications such as CNC machines, where the tool is required to move along a pre-planned path with high speed and precision, vibration is a common issue that can lead to degradation of positional accuracy. This issue is addressed with the help of trajectory planning, where the implementation of an S-curve trajectory is reported to result in high positional accuracy compared to a trapezoidal velocity trajectory. This paper introduces the different properties of fourth-order symmetrical S-curve trajectory for the point-to-point motion transfer system. Complex mathematics is required to acquire the desired values of motion parameters of the trajectory. Therefore, the paper proposes a novel unitization approach that treats time and displacement as one unit each and simplifies the complex mathematics. This method provides a single generalized solution for any displacement and motion time value. The paper illustrates graphical relationships among motion parameters such as peak values of velocity, acceleration, jerk, and snap, which can serve as nomograms for choosing appropriate values to design displacement trajectories. Using these graphs, the paper outlines simple guidelines for selecting suitable values of motion parameters adapted to common situations. Finally, a case study is presented to validate feasibility of the proposed method.

Keywords: *Critical motion parameter, Multiplication factor, Velocity, Unitized value*

1. Introduction

Trajectory planning plays a key role in obtaining high speed and precision in point-to-point motion transfer applications such as robots and CNC machinery. The trajectory planning includes a control algorithm created using motion trajectories. The trapezoidal velocity trajectory is the fastest trajectory used in a point-to-point motion transfer application. However, this trajectory generates a large jerk force that causes the generation of vibration and degradation of positional accuracy. S-curve trajectories are introduced to overcome the limitation of the trapezoidal velocity trajectory [1]–[4]. This trajectory can provide smoother point-to-point motion, which helps in improving the positional accuracy and reducing the vibration.

The S-curve trajectory is studied by researchers aiming to enhance controller performance in point-to-point motion transfer applications [5]–[7]. Meckl et al. present a third-order S-curve trajectory, where a ramp-up time is optimized to minimize the vibration in a flexible system [8]. A parameter, jerk ratio [9]–[11], and jerk period ratio [12], [13] are presented for designing the third-order asymmetrical S-curve trajectory to produce a lower vibration amplitude in the flexible system. Fast acceleration and slow retardation third-order asymmetrical S-curve trajectory is introduced to obtains the desired position with a minimum vibration and lower positioning time [14]–[16]. A new freeform third-order asymmetrical S-curve trajectory is presented to effectively suppresses the vibration and minimizes the settling time of the flexible motion system [17]. Chen et al. present a look-ahead algorithm, demonstrating its effectiveness to minimize machining time and smoothing motion in CNC machines [18]. Lu and Chen present a genetic algorithm for trajectory planning in a five-axis machine tool, achieving higher machining speeds without violating axis motion limits [19].

From preceding discussion, it can be concluded that utilizing a third-order S-curve trajectory, raises the performance of the system. Furthermore, for achieving highly precise point-to-point motion, smoothness emerges as a crucial criterion that can avoid unwanted mechanical disturbances and improve performance of the controller. Hence, the trajectory order should be raised to further increase the smoothness in a motion [20]. Lambrechts et al. introduced a new algorithm for designing the time-optimal fourth-order symmetrical S-curve trajectory, aiming to minimize servo error and achieve zero-settling behavior [21]. A time optimization algorithm is presented to obtain high accuracy for the end position in a CNC simulation system [22]. Fan et al. present the different properties of a fourth-order symmetrical S-curve trajectory [23]. The properties are used to create the time-optimal algorithm for minimizing the vibration in the CNC machine [23]. In [24], an optimized fourth-order symmetrical S-curve trajectory is presented for a specific time requirement to minimize the residual vibration in a flexible system. Lee and Ha present an optimization algorithm to design an optimum fourth-

[1] *Visvesvaraya National Institute of Technology, Nagpur – 440010, India*
ORCID ID : 0000-0002-8296-0210
[2] *Visvesvaraya National Institute of Technology, Nagpur – 440010, India*
ORCID ID : 0000-0002-0764-4971
[3] *Visvesvaraya National Institute of Technology, Nagpur – 440010, India*
** Corresponding Author Email: rupeshtatte0096@gmail.com*

order symmetrical S-curve trajectory for achieving low residual vibration and fast movement in a flexible system [25]. Various guidelines are given to obtain the best order of a trajectory for a given motion system under various performance evaluation criteria [25].

Most of the mentioned research focuses solely on planning time-optimal third-order S-curve trajectories. The trajectories are designed considering the limiting value of velocity, acceleration, and jerk. There are limited studies that address the planning of fourth-order S-curve trajectories. The solutions reported often involve complex mathematics and only offer minimum-time solutions, which may not be feasible for achieving higher smoothness in the point-to-point motion. Furthermore, the detailed analysis of fourth-order symmetrical S-curve trajectory is not addressed in the aforementioned literature. Such characterization is valuable for determining the desired values of motion parameters for specific time and displacement.

This paper presents different nomograms to obtain the desired chracteristics of the fourth-order symmetrical S-curve trajectory. The nomograms aid to acquire the desired and feasible chracteteristics of the trajectory without using the complex computaion. Quantitative evauation through visual analysis is the primary merit of the presented nomograms. The feasible combination of values of peak velocity, acceleration, jerk, and snap can easily choose without entering into complex calculations using the provided graphs. The graphs are created using the novel unitization method which treats time and displacement as one unit each. The choosen unitized values can be transform to actual values using the multiplication factors. The practicality of the presented approach is validated using a case study. The presented nomograms can also be utilized to determine the desired combination of values for a third-order symmetrical S-curve trajectory.

The paper is categorized as follows: The procedure for designing a fourth-order symmetrical S-curve trajectory is outlined in Section 2. Section 3 presents the analysis of a unitized fourth-order S-curve trajectory. In Section 4, a numerical example is provided. At the end, the conclusions are written in Section 5.

2. Fourth-Order Trajectory Planning

The fourth-order symmetrical S-curve trajectory is shown in Fig. 1. It comprises 15 segments: one constant velocity, two constant acceleration, four constant jerk, and eight constant snap. The time durations of constant velocity, acceleration, jerk, and snap are represented by $\Delta t_v \in [t_7, t_8]$, $\Delta t_a \in [[t_3, t_4], [t_{11}, t_{12}]]$, $\Delta t_j \in [[t_1, t_2], [t_5, t_6], [t_9, t_{10}], [t_{13}, t_{14}]]$, and $\Delta t_s \in [[t_0, t_1], [t_2, t_3], [t_4, t_5], [t_6, t_7], [t_8, t_9], [t_{10}, t_{11}], [t_{12}, t_{13}], [t_{14}, t_{15}]]$, respectively. For these 15 segments, the total motion time is determined as $T = 8\Delta t_s + 4\Delta t_j + 2\Delta t_a + \Delta t_v$.

In Fig. 1, s represents the peak value of snap. Similarly, j, a, v, and d represents the peak value of jerk, acceleration, velocity and displacement, respectively. The snap trajectory is expressed by the fomulations provided in (1). This trajectory is expressed with j and Δt_s as variables.

$$s(t)=\begin{cases} \dfrac{j}{\Delta t_s} & 0\le t\le t_1,\ t_6\le t\le t_7,\ t_{10}\le t\le t_{11},\ t_{12}\le t\le t_{13} \\ 0 & t_1\le t\le t_2,\ t_3\le t\le t_4,\ t_5\le t\le t_6,\ t_7\le t\le t_8, \\ & t_9\le t\le t_{10},\ t_{11}\le t\le t_{12},\ \ t_{13}\le t\le t_{14} \\ -\dfrac{j}{\Delta t_s} & t_2\le t\le t_3,\ t_4\le t\le t_5,\ t_8\le t\le t_9,\ t_{14}\le t\le t_{15} \end{cases} \tag{1}$$

where $s(t)$ represents the snap for a given time.

The equations for the jerk trajectory $j(t)$ can be obtained by integrating (1) once for a given time.

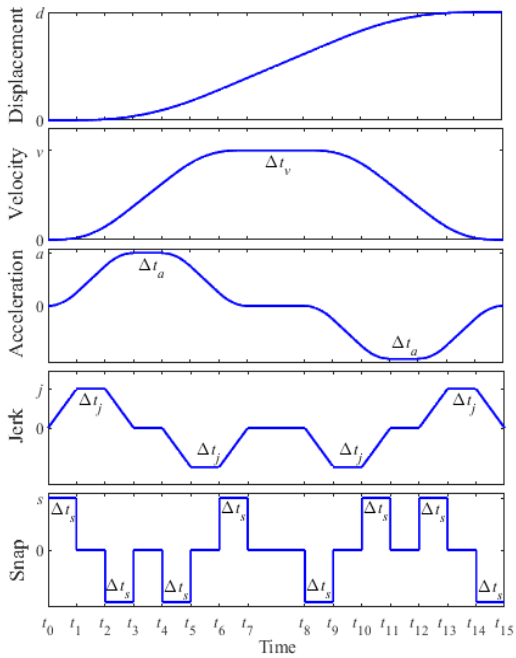

Fig. 1. Fourth-order symmetrical S-curve trajectory.

Motion parameters	Velocity	Acceleration	Jerk	Snap
Multiplication factor	$\frac{P_1}{P_2}$	$\frac{P_1}{{P_2}^2}$	$\frac{P_1}{{P_2}^3}$	$\frac{P_1}{{P_2}^4}$

$$
j(t) = \begin{cases}
\frac{jt}{\Delta t_s} & t_0 \le t \le t_1 \\
j & t_1 \le t \le t_2,\quad t_{13} \le t \le t_{14} \\
\frac{j(2\Delta t_s + \Delta t_j - t)}{\Delta t_s} & t_2 \le t \le t_3 \\
0 & t_3 \le t \le t_4,\ t_7 \le t \le t_8, \\
 & t_{11} \le t \le t_{12} \\
\frac{j(2\Delta t_s + \Delta t_j + \Delta t_a - t)}{\Delta t_s} & t_4 \le t \le t_5 \\
-j & t_5 \le t \le t_6,\quad t_9 \le t \le t_{10} \\
\frac{j(t - 4\Delta t_s - 2\Delta t_j - \Delta t_a)}{\Delta t_s} & t_6 \le t \le t_7 \\
\frac{j(4\Delta t_s + 2\Delta t_j + \Delta t_a + \Delta t_v - t)}{\Delta t_s} & t_8 \le t \le t_9 \\
\frac{j(t - 6\Delta t_s - 3\Delta t_j - \Delta t_a - \Delta t_v)}{\Delta t_s} & t_{10} \le t \le t_{11} \\
\frac{j(t - 6\Delta t_s - 3\Delta t_j - 2\Delta t_a - \Delta t_v)}{\Delta t_s} & t_{12} \le t \le t_{13} \\
\frac{j(8\Delta t_s + 4\Delta t_j + 2\Delta t_a + \Delta t_v - t)}{\Delta t_s} & t_{14} \le t \le t_{15}
\end{cases} \tag{2}
$$

The equations for the acceleration trajectory *a*(*t*), velocity trajectory *v*(*t*), and displacement trajectory *d*(*t*) can be established by integrating (2) once, two times, and three times for a given time.

2.1. Unitization of Fourth-Order S-curve Trajectory

A novel unitization method is presented to generalize the point-to-point motion by treating displacement and time as one unit ($d = T = 1$). The purpose of this method is to provide a general solution that can be used with any type of point-to-point motion transfer application used in the industrial field. The desired solution can be worked out and selected from the plots generated by this method.

The fourth-order S-curve trajectory expressed by this method is referred to here as a unitized fourth-order S-curve trajectory. The values of motion parameters are defined here as unitized values. The multiplication factors, given in Table 1, are used to transform the unitized value into actual values. The actual values can be obtained by multiplying the unitized values by given multiplication factors, where P_1 is the actual displacement and P_2 is the actual motion time.

Table 1. Multiplication factors

Conventional constant velocity, constant acceleration, constant jerk, and constant snap trajectories are the unique cases of the fourth-order S-curve trajectory. These conventional trajectories are used to determine the minimum peak values of motion parameters. The minimum peak value of *v*, *a*, *j*, and *s* are determined using constant velocity, constant acceleration, constant jerk, and constant snap trajectory, respectively. The unitized minimum peak value of *v*, *a*, *j*, and *s* are 1 unit, 4 units, 32 units, and 512 units, respectively. The maximum peak value of *a*, *j*, and *s* can increase to infinity, whereas *v* can only rise to 2 units.

3. Analysis of Unitized Fourth-Order S-Curve Trajectory

The values of *a*, *j*, and *s* can rise to infinity, while the value of *v* can only rise to 2 units. With increase in the value of *v*, the values of the other motion parameters decrease. If the value of *v* is maintained at 2 units, the other motion parameter's values will automatically reduce. Therefore, two separate analyses are conducted, one is by considering maximum value of *v*, i.e., 2 units, and another is by considering all possible values of *v* from 1 unit to 2 units.

3.1. Analysis at Maximum Value of Velocity

To study the effect of various motion parameters on each other a graph is plotted, as shown in Fig. 2, between peak acceleration and jerk. Each curve in the graph shows the specific value of *s*. This study is conducted while maintaining velocity at its maximum value of 2 units. The graph is drawn to visually analyze the relationship between the values of *a*, *j*, and *s* for 2 units of *v*. Each and every feasible magnitude of *a*, *j*, and *s* can be visualized in the narrow band. At point A on the graph, a minimum *s* value of 512 units is achieved. At this point the value of *v* is 2 units, *a* is 8 units, and *j* is 64 units. These values of *v*, *a* and *j* are two times their minimum values.

When the value of *s* is permitted to be double its minimum value, and the values of both *v* and *a* are maintained at double their respective minimum values, the value of jerk *j* decreases to 1.18 times its minimum value, i.e.,37.6 units. The value is shown in Fig. 2 at point B. Further, when the value of *s* is raised to 4 times its minimum value, the value of *j* decreases to 1.08 times its minimum value, i.e., 34.4 units. The value is shown at point C in Fig. 2. The blue curve at the bottom in Fig. 2 represents the values of *a* and *j* for a third-order S-curve trajectory. Point D on that curve represents the minimum value of *j*, i.e., 32 units. At this point, the value of *a* reaches to 8 units and *s* reaches to infinity. At the left end of the bottom blue curve represents the minimum value of *a*, i.e., 4 units. At this minimum value of *a*, the value of both *j* and *s* reaches to infinity.

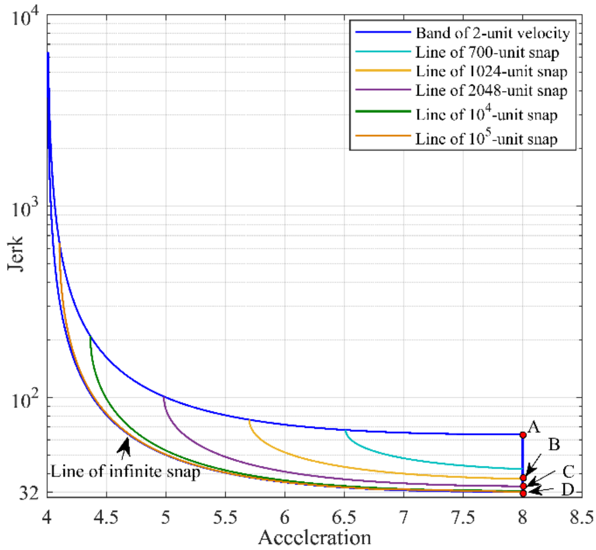

Fig. 2. Graph for peak velocity of 2 units.

3.1.1. When Acceleration is Critical

When the acceleration is given importance, and its value is raised to 5 units, 25% higher value than its minimum, the value of *j* varies between 50 units and 100 units, and the value of *s* is lowered by up to 2000 units, as shown in Fig. 2. Allowing the value of *a* to be 25% higher than its minimum value leads to drastic declines in the values of both *j* and *s* from infinity to values only slightly higher than their minimum values.

3.1.2. When Acceleration is More Critical

When the acceleration is more critical, permitting a value of 4.5 units, 12.5% higher than its minimum value, the value of *j* varies between 81 units and 162 units, and *s* experiences a reduction of up to 6000 units, as shown in Fig. 2. Even with a 10% increase in *a*, i.e., 4.4 units, *j* will be within 200 units, but *s* will be high around 10^4 or more units, and with a 5% increase in *a*, i.e., 4.2 units, *j* will be within 500 units, but *s* will be very high around 10^5 units.

This shows that any further reduction in the value of *a* increases the values of a *j* and *s*, rather *s* increases exponentially. Based on this observation, if a value of *v* of 2 units is allowed and the values of *s* and *j* are important but not critical, permitting a value from 4.4 units to 5 units is an acceptable compromise for managing the values of *s* and *j*. Nevertheless, if snap and acceleration are important and jerk is considered critical and, or if acceleration is important and both snap and jerk are considered critical, it is advisable to raise the value of *a* to around 8 units.

3.1.3. When Jerk is Critical

When jerk is considered critical, and its value is raised to 40 units, 25% higher than its minimum value, the value of *a* varies between 5.5 units and 8 units, and the value of *s* is lowered up to 800 units. Therefore, permitting the value of *j* to be 25% higher than its minimum value results in a drastic reduction in the values of both *a* and *s*.

3.2. Analysis for All Possible Values of Velocity

To minimize the value of any critical motion parameter, it is required to maintain the value of *v* close to its maximum value, i.e., 2 units. However, selecting maximum value of *v* reduces the value of only one motion parameter and increases the values of others. Hence, this section analyzes the effect of all the possible values of *v* on the values of *a*, *j*, and *s*. Fig. 3 shows different graphs plotted between acceleration and jerk for different *v* from 1.1 units to 2 units with lines representing corresponding *s* values. These plots show the complete solution for selecting the combinations of values of motion parameters. The bottom curve in each plot provides the values of *a* and *j* for the third-order S-curve trajectory.

When permitting 1.4 units value of *v*, the minimum values of *j* and *a* are decreased from infinity to 68.48 units and 4.92 units, respectively, as shown in Fig. 3(d). Furthermore, when the value of *v* is permitted to be 1.3 units, the values of *a* and *j* are decreased from infinity to 5.64 units and 97.6 units, respectively, as shown in Fig. 3(c). A drastic increase in the values of *a* and *j* is observed as compared to the values at a *v* of 1.4 units. If *v* is permitted beyond 1.4 units, a reduction in *a* will not be substantial, but if *v* is tried to be reduced, *a* will increase substantially. A similar trend is observed even for *j*.

3.2.1. When Acceleration is Critical

When the acceleration is critical and permitted 25% more value than its minimum value, the value of *v* needs to be raised by more than 1.4 units. For the similar permitted value of *a*, and *v* of 1.6 units, 1.8 units, and 2 units, the value of *j* is decreased to 64 units, 59.2 units, and 50.2 units, respectively, and the value of *s* is decreased to 12.5, 5.5, and 4 times its minimum value, respectively. This significant decline in the values of *s* and *j* can be accepted when both snap and jerk are important but not critical. Furthermore, at a *v* of 1.5 units and 1.4 units, the *j* is decreased to 144 units and 816 units, respectively, and *s* is decreased to 34 and 2000 times its minimum value, as shown in Fig. 3(a) and Fig. 3(d). This reasonable decline in the values of *s* and *j* cannot be accepted even when both snap and jerk are important. Hence, when acceleration is critical and only permitted 5 units, and snap and jerk are important, it is required to utilize the value of *v* more than 1.6 units. The value of both *j* and *s* substantially increases for any further reduction in the value of *v*.

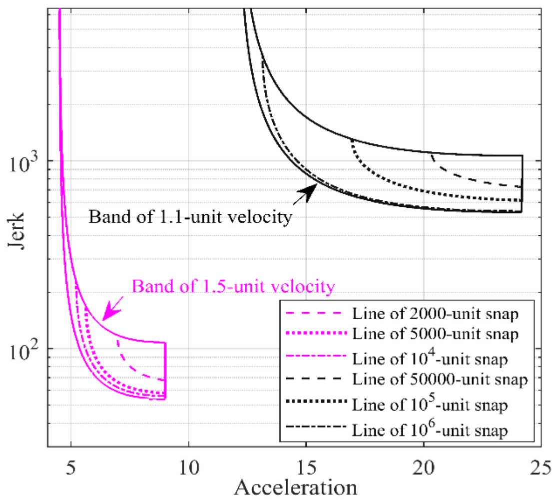

(a)

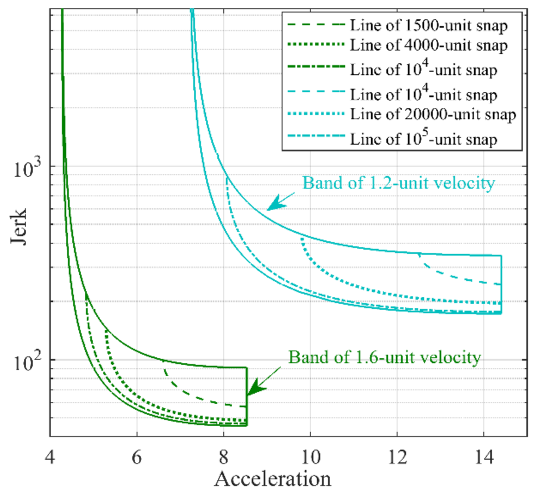

(b)

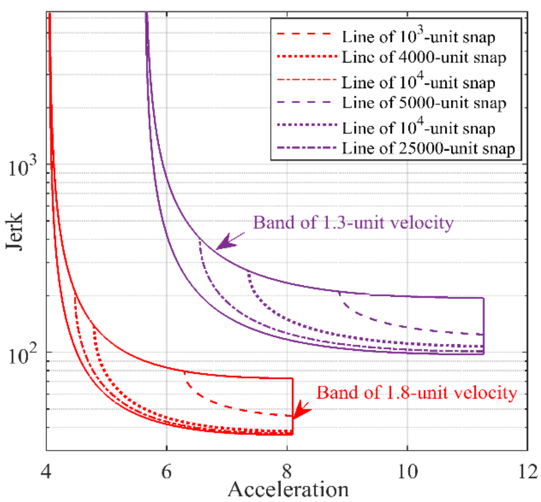

(c)

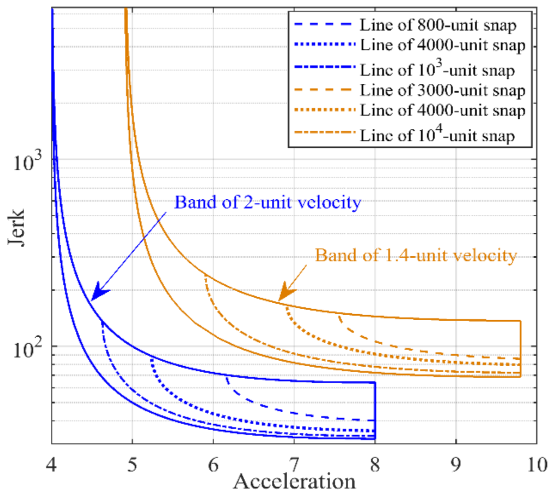

(d)

Fig. 3. Graphs for the peak velocity of (a) 1.1 units and 1.5 units, (b) 1.2 units and 1.6 units, (c) 1.3 units and 1.8 units and (d) 1.4 units and 2 units.

3.2.2. When Jerk is Critical

When the value of *j* is permitted to be 40 units, the value of *v* must be equal to or greater than 1.8 units. For the similar permitted value of *j*, and *v* of 1.8 units, the values of *s* and *a* are decreased to around 4 and 2 times their minimum values, respectively, as shown in Fig. 3(c). This reasonable decline in the values of *s* and *a* can be accepted when both snap and acceleration are important but not critical. As a result, when the jerk is considered critical, and other motion parameters are considered important, there is no need to use the *v* of 2 units. The value of *j* can be reduced to 40 units, even with the use of 1.8 units of *v*. It is also observed that if the value of *j* decreases further, the value of *v* will increase beyond 1.8 units.

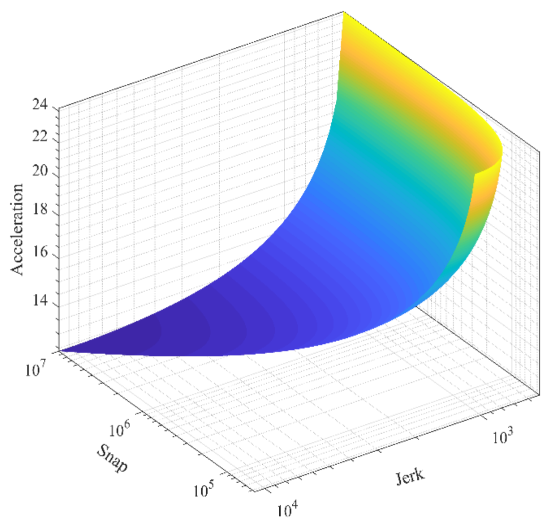

(a)

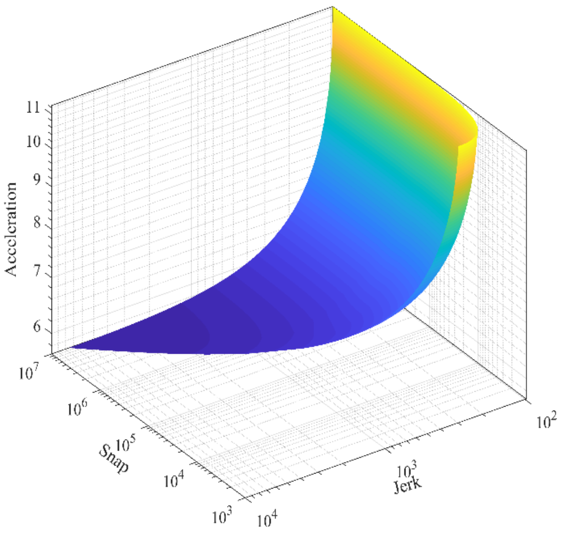

(b)

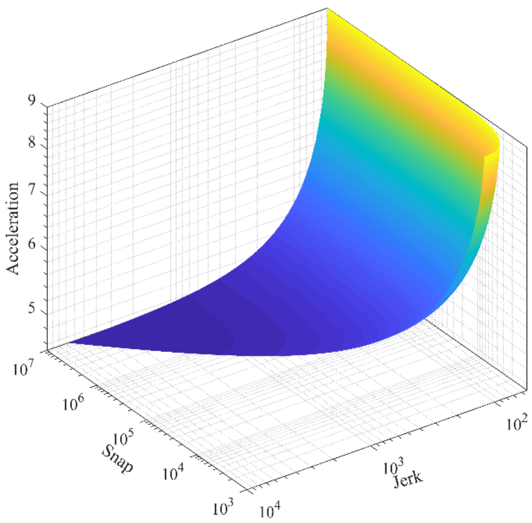

(c)

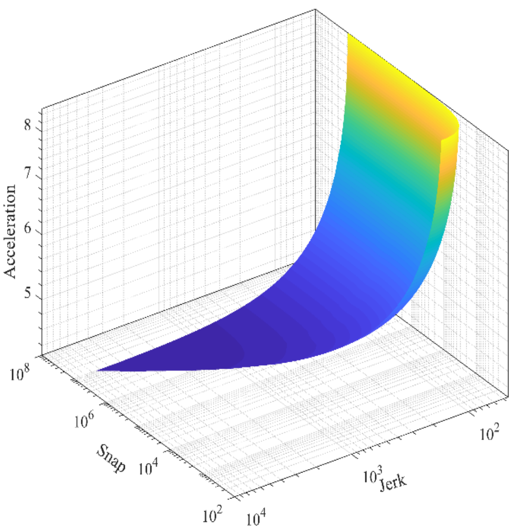

(d)

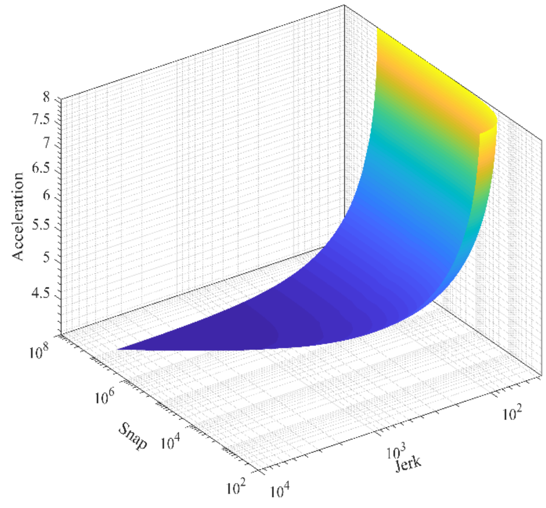

(e)

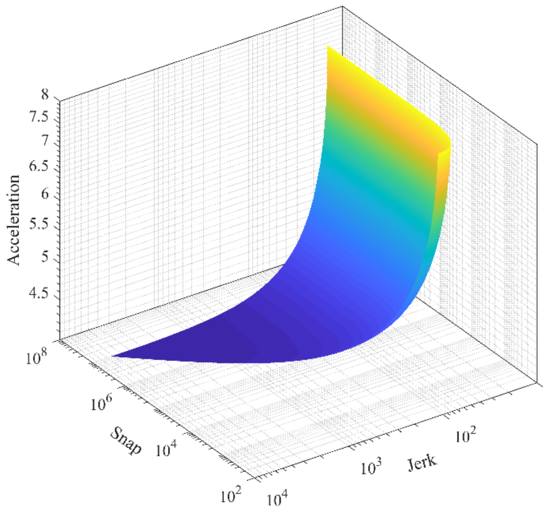

(f)

Fig. 4. 3-dimenstion surface plots for the peak velocity of (a) 1.1 units, (b) 1.3 units, (c) 1.5 units, (d) 1.6 units, (e) 1.8 units, and (f) 2 units.

In the above analysis, only acceleration and jerk are considered as critical motion parameters, with velocity being ignored. If velocity is considered critical and permitted about 1.2 units of *v*, the values of *a*, *j*, and *s* rise excessively, as shown in Fig. 3(b). Nevertheless, if this much of a rise in the values of *a*, *j*, and *s* is allowed, a *v* of value 1.2 units and even 1.1 units can be utilized.

Fig. 4 shows the 3-dimension surface plot illustrating the relationship between acceleration, jerk, and snap for different peak velocities. Similar patterns are observed in these plots as seen in Fig. 3. The dark blue color represents lower *a*, and the yellow color indicates higher *a*. Figs. 2, 3, and 4 can be used as a nomogram for visually selecting, without entering into any calculation, a feasible combination of unitized values of *v*, *a*, *j*, and *s* when the limiting values of motion parameters, i.e., v_{max}, a_{max}, j_{max}, and s_{max}, are known. A good combination based on the requirements can be found quickly.

4. Numerical Example

A case study is conducted to validate the practicality of a unitized fourth-order symmetrical S-curve trajectory. As an example, the actual displacement is given as d = 1.2 meters and the actual motion time is considered as T = 2 sec. The value of P_1 and P_2 is 1.2 meters and 2 sec, respectively. The multiplication factors and corresponding unitized and actual minimum values of motion parameters for a given value of P_1 and P_2 are presented in Table 2.

Let's consider, the limiting values of actuator as v = 0.96 m/sec (unitized value = 1.6 units) and a = 1.92 m/sec^2 (unitized value = 6.4 units). If a minimum value of s is needed for given limiting values of v and a, Fig. 5 gives the approximate values of s and j as 1640 units and 102 units, respectively. These values can be visualized at point A, providing actual value of s and j as 123 m/sec^4 and 15.3 m/sec^3. When the minimum value of j is needed rather than the value of s, the fourth-order S-curve trajectory is converted to the third-order S-curve trajectory. It occurs because s increases to infinity at a minimum value of j. The minimum value of j can be visualized at point D in Fig. 5 as 51 units, providing an actual j of 7.65 m/sec^3.

Table 2. Values of motion parameters for a given case study

Motion parameters	v	a	j	s
Unitized minimum peak values	1	4	32	512
Multiplication factor	$\frac{P_1}{P_2}$ -0.6	$\frac{P_1}{P_2^2}$ -0.3	$\frac{P_1}{P_2^3}$ -0.15	$\frac{P_1}{P_2^4}$ -0.075
Actual minimum peak value	0.6 m/sec	1.2 m/sec^2	4.8 m/sec^3	38.4 m/sec^4

Now, if the limiting value of j is also provided as 9.6 m/sec^3 (64 - unitized value) along with limiting values of v and a, and the minimum value of s is needed, Fig. 5 provides 2560 units of s value, giving 192 m/sec^4 as an actual s. These values can be visualized at point B in Fig. 5. If the limiting value of s is provided as 360 m/sec^4 (4800 - unitized value) instead of a limiting value of j, and a minimum value of j is needed, Fig. 5 provides 56 units of j value as shown at point C, giving 8.4 m/sec^3 as an actual j.

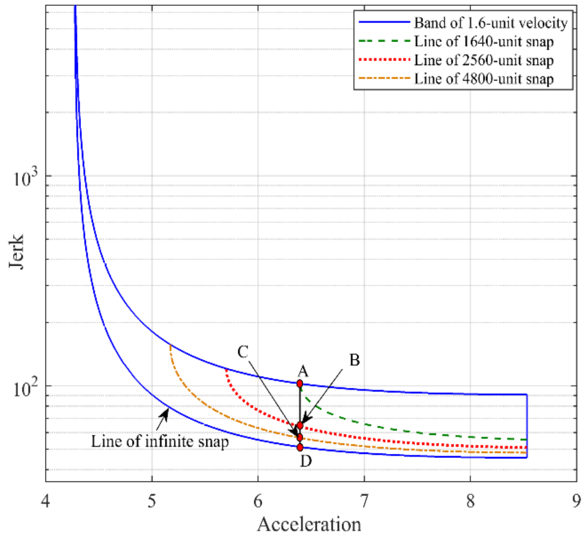

Fig. 5. Graph for the peak velocity of 1.6 units.

5. Conclusions

This paper presents different characteristics of the fourth-order symmetrical S-curve trajectory using the novel unitization method. The characteristics are expressed in the form of nomograms that can be utilized to obtain the desired values of motion parameters for a point-to-point motion system. The nomograms are provided to qualitatively manipulate the values of motion parameters. Detailed analysis of the trajectory is conducted by using the proposed nomograms. In the analysis, different critical criteria are elaborated. A desired and feasible combination of values of motion parameters can be quickly found without any calculations using the proposed nomograms. A case study is presented to validate the practicability of the proposed method of unitization.

Based on the given analysis, following important conclusions are drawn:

1) The plots in Figs. 2, 3, and 4 are suitable for qualitatively manipulating the values of v, a, j, and s and are useful for trajectory planning. The figures can be utilized as nomograms for third and fourth-order trajectories.
2) The values of j, a, and v need to be raised two times their minimum values, i.e., 64 units, 8 units, and 2 units, to attain the minimum value of s of 512 units. These are well-established values. They are re-established for unitized model.
3) If the maximum value of v, i.e., 2 units, is permitted, the values of a, j, and s can be easily controlled. In this case, just permitting a of 5 units, the value of j is reduced drastically between 50 units to 100 units, and s is decreased up to 2000 units.
4) By permitting the value of j 25% higher than its minimum value and v to be maintained at 2 units, the values of a and s can be easily controlled.
5) The values of a and j drastically increase if v falls below 1.4 units,

6) The provided plots are useful for selecting the appropriate combination of values of motion parameters within the given drive limitations (limiting values of motion parameters).

Author contributions

Rupesh Tatte1: Methodology, Software, Conceptualization, Field study **Hemant Jawale2:** Writing-original draft preparation, Data curation, Field study, Software **Hemant Thorat3:** Investigation, Visualization, Writing-Reviewing and Editing.

Conflicts of interest

The authors have no conflicts of interest to declare.

References

[1] H. Z. Li, Z. M. Gong, W. Lin, and T. Lippa, "Motion profile planning for reduced jerk and vibration residuals," *SIM Tech*, vol. 8, pp. 32-37, 2015.

[2] S. Perumaal and N. Jawahar, "Synchronized trigonometric S-curve trajectory for jerk-bounded time-optimal pick and place operation," *Int J Robot Autom*, vol. 27, no. 4, pp. 385–395, 2012.

[3] K. D. Nguyen, T. C. Ng, and I. M. Chen, "On Algorithms for Planning S-Curve Motion Profiles," *Int J Adv Robot Syst*, vol. 5, no. 1, pp. 99–106, 2008.

[4] H. Ouyang, J. Hu, G. Zhang, L. Mei, and X. Deng, "Decoupled linear model and S-shaped curve motion trajectory for load sway reduction control in overhead cranes with double-pendulum effect," *Proc Inst Mech Eng Part C J Mech Eng Sci*, vol. 233, no. 10, pp. 3678–3689, 2019.

[5] H. Ding, S. Member, and J. Wu, "Point-to-Point Motion Control for a High-Acceleration Positioning Table via Cascaded Learning Schemes," *IEEE Trans Ind Electron*, vol. 54, no. 5, pp. 2735–2744, 2007.

[6] K. Erkorkmaz and Y. Altintas, "High speed CNC system design . Part I : jerk limited trajectory generation and quintic spline interpolation," *Int. J Mach Tools Manuf*, vol. 6955, pp. 2–5, 2001.

[7] J. R. Garcia Martinez, J. Rodriguez Resendiz, M. A. Martinez Prado, and E. E. Cruz Miguel, "Assessment of jerk performance s-curve and trapezoidal velocity profiles," *13th Int Eng Congr*, 2017.

[8] P. H. Meckl, P. B. Arestides, and M. C. Woods, "Optimized S-curve motion profiles for minimum residual vibration," *Proc Am Control Conf*, vol. 5, pp. 2627–2631, 1998.

[9] K. H. Rew and K. S. Kim, "A closed-form solution to asymmetric motion profile allowing acceleration manipulation," *IEEE Trans Ind Electron*, vol. 57, no. 7, pp. 2499–2506, 2010.

[10] [10] C. W. Ha, K. H. Rew, and K. S. Kim, "A complete solution to asymmetric S-curve motion profile: Theory & experiments," *Int Conf Control Autom Syst*, pp. 2845–2849, 2008.

[11] [11] K. H. Rew and K. S. Kim, "Using asymmetric S-curve profile for fast and vibrationless motion," *Int Conf Control Autom Syst*, pp. 500–504, 2007.

[12] [12] K. H. Rew, C. W. Ha, and K. S. Kim, "A practically efficient method for motion control based on asymmetric velocity profile," *Int J Mach Tools Manuf*, vol. 49, no. 7–8, pp. 678–682, 2009.

[13] C. W. Ha, K. H. Rew, and K. S. Kim, "Robust zero placement for motion control of lightly damped systems," *IEEE Trans Ind Electron*, vol. 60, no. 9, pp. 3857–3864, 2013.

[14] D. M. Tsay and C. F. Lin, "Asymmetrical inputs for minimizing residual response," *IEEE Int Conf Mechatronics*, pp. 235–240, 2005.

[15] F. Zou, D. Qu, and F. Xu, "Asymmetric s-curve trajectory planning for robot point-to-point motion," *IEEE Int Conf Robot Biomimetics*, pp. 2172–2176, 2009.

[16] R. Bearee and A. Olabi, "Dissociated jerk-limited trajectory applied to time-varying vibration reduction," *Robot Comput Integr Manuf*, vol. 29, no. 2, pp. 444–453, 2013.

[17] Y. Bai, X. Chen, H. Sun, and Z. Yang, "Time-Optimal Freeform S-Curve Profile under Positioning Error and Robustness Constraints," *IEEE/ASME Trans Mechatronics*, vol. 23, no. 4, pp. 1993–2003, 2018.

[18] Y. Chen, X. Ji, Y. Tao, and H. Wei, "Look-ahead algorithm with whole s-curve acceleration and deceleration," *Adv Mech Eng*, vol. 5, pp. 1-9, 2013.

[19] T. C. Lu and S. L. Chen, "Genetic algorithm-based S-curve acceleration and deceleration for five-axis machine tools," *Int J Adv Manuf Technol*, vol. 87, no. 1–4, pp. 219–232, 2016.

[20] Y. Fang, J. Hu, W. Liu, Q. Shao, J. Qi, and Y. Peng, "Smooth and time-optimal S-curve trajectory planning for automated robots and machines," *Mech Mach Theory*, vol. 137, pp. 127–153, 2019.

[21] P. Lambrechts, M. Boerlage, and M. Steinbuch, "Trajectory planning and feedforward design for electromechanical motion systems," *Control Eng Pract*, vol. 13, pp. 145–157, 2005.

[22] F. Song, S. Yu, and T. Chen, "Research on CNC simulation system with instruction interpretations possessed of wireless communication," *J Supercomput*, vol. 72, pp. 2703–2719, 2016.

[23] W. Fan, X. S. Gao, W. Yan, and C. M. Yuan, "Interpolation of parametric CNC machining path under confined jounce," *Int J Adv Manuf Technol*, vol. 62, no. 5–8, pp. 719–739, 2012.

[24] R. Tatte, H. Thorat, and H. Jawale, "Optimization of higher - order S - curve motion profile using unitization method aiming to reduce the vibration of a lightly damped system," *J Brazilian Soc Mech Sci Eng*,

vol. 46, no. 183, pp. 1-28, 2024.
[25] D. Lee and C. W. Ha, "Optimization process for polynomial motion profiles to achieve fast movement with low vibration," *IEEE Trans Control Syst Technol*, vol. 28, no. 5, pp. 1892–1901, 2020.